AIP | Applied Physics Letters

Acoustic particle palpation for measuring tissue elasticity

Hasan Koruk, Ahmed El Ghamrawy, Antonios N. Pouliopoulos, and James J. Choi

Citation: Applied Physics Letters **107**, 223701 (2015); doi: 10.1063/1.4936345
View online: http://dx.doi.org/10.1063/1.4936345
View Table of Contents: http://scitation.aip.org/content/aip/journal/apl/107/22?ver=pdfcov
Published by the AIP Publishing

Acoustic particle palpation for measuring tissue elasticity

Hasan Koruk,[1,2] Ahmed El Ghamrawy,[1] Antonios N. Pouliopoulos,[1] and James J. Choi[1,a)]
[1]*Noninvasive Surgery and Biopsy Laboratory, Department of Bioengineering, Imperial College London, London SW7 2AZ, United Kingdom*
[2]*Mechanical Engineering Department, MEF University, Istanbul 34396, Turkey*

(Received 13 August 2015; accepted 11 November 2015; published online 1 December 2015)

We propose acoustic particle palpation—the use of sound to press a population of acoustic particles against an interface—as a method for measuring the qualitative and quantitative mechanical properties of materials. We tested the feasibility of this method by emitting ultrasound pulses across a tunnel of an elastic material filled with microbubbles. Ultrasound stimulated the microbubble cloud to move in the direction of wave propagation, press against the distal surface, and cause deformations relevant for elasticity measurements. Shear waves propagated away from the palpation site with a velocity that was used to estimate the material's Young's modulus.
[http://dx.doi.org/10.1063/1.4936345]

Palpation—the application of pressure against a material's surface—and monitoring of the deformation or force response are effective in determining a material's mechanical properties.[1–5] In the lab and the clinic, this two-part process is used in the diverse and complex range of elasticity measurement devices available.[6–8] Optical[9] and magnetic[10] tweezers use particles responsive to light or magnetism, respectively, to apply stress. In the clinic, manual palpation of superficial tissue provides a qualitative assessment of stiffness and is used to diagnose diseases, such as breast cancer. In order to assess deeper tissues, an ultrasound beam is used to palpate by exerting an acoustic radiation force (ARF) in the direction of propagation.[11] Palpation is the fundamental basis of these elasticity measurement systems and the characteristics of the stress source determine the capabilities and limitations of the system.

In contrast to other stress sources, ultrasound has the unique ability to palpate areas beneath the surface of materials by focussing the beam to a region of interest. Physical objects press directly against the surface of a material. On the other hand, ultrasound propagates through the material while momentum is transferred from the acoustic wave onto the material through absorption, scattering, and reflection. Thus, ARF-induced stress is applied not from the surface of a material, but throughout a long ellipsoidal beam volume that is typically on the order of a few millimetres wide and tens of millimetres long. This larger stress volume makes conventional elastography more susceptible to a breakdown of the assumptions of tissue homogeneity—in other words, there is uncertainty regarding the ARF-induced stress distribution within a beam, because it is dependent on the material's unknown acoustic properties such as absorption and reflection coefficients. Complications arise in materials with lesions, layers, vessels, cavities, etc. Although ARF-based ultrasound elasticity imaging has been used in the clinic (e.g., diagnosis of diffuse liver diseases[12] and breast masses[13]), there is a need to improve the contrast and spatial resolution of elasticity imaging.[8] This may be overcome by a smaller and higher magnitude stress source that can be applied deep into tissue.

Our proposed method takes advantage of a well-known interaction between ultrasound and microbubbles known as the primary ARF. Lipid-shelled microbubbles with a stabilised gas core are used regularly in the clinic as an ultrasound imaging contrast agent (e.g., SonoVue® and Definity®). When exposed to ultrasound, microbubbles undergo volumetric oscillations due to their compressibility and scatter the incident wave. When driven at their resonance frequency, microbubbles experience a higher radiation force compared to soft tissue.[14] A single bubble pushed by ultrasound has been previously shown to cause local tissue deformation. Ultrasound can push a large bubble (diameter: 100–800 μm) embedded inside an elastic material to derive elasticity values.[14] This technique used a high-powered laser to generate this bubble, which limits its application to shallow targets and requires local destruction of the material, which may not be permissible in human tissue. In a separate study that investigated the mechanisms of clot lysis using ultrasound and microbubbles, indentation of fibrin clots was observed.[15] However, the deformation was induced by a single microbubble and for fibrin clots that are softer than most organs. Currently, there is no physiologically relevant method for using microbubbles as a stress source for measuring tissue elasticity.

We propose palpation with a population of acoustic particles as a stress source for measuring qualitative and quantitative elasticity values. Ultrasound alone deforms a large internal volume of a material. In contrast, we will explore the use of multiple microbubbles pushed by ultrasound to press upon internal surface of materials (i.e., fluid-tissue interfaces). This technique has the potential to palpate at a magnitude, scale, distribution, and depth that are currently unachievable with ARF alone. We will demonstrate the feasibility of acoustic particle palpation using ultrasound and lipid-shelled microbubbles, and although this technique has a wide range of applications, we will demonstrate its

a)Author to whom correspondence should be addressed. Electronic mail: j.choi@imperial.ac.uk

physiological relevance using tissue-mimicking phantoms with elastic properties similar to in vivo tissue.

A gelatin-based tissue-mimicking material containing a wall-less tunnel (diameter: 800 μm) was immersed in a water tank. Lipid-shelled microbubbles with a stabilised gas core (diameter: 1.32 ± 0.76 μm) were administered into the tunnel so that they were compartmentally separate from the surrounding material (Fig. 1). Focused ultrasound pulses were emitted from a single-element transducer [centre frequency (f_c): 5 MHz], which was driven by a function generator through a power amplifier. The centre frequency was selected to match the resonance frequency of the microbubbles in order to maximise the generated force. Deformations of the tunnel wall were measured with high-speed optical microscopy (frame rate: 1.2 kHz). The microbubble manufacturing process and experimental hardware are described in the supplementary material.[16]

Ultrasound was applied [peak-negative pressure (p_n): 625 kPa, pulse length (PL): 40 ms] on a wall-less tunnel phantom (2.5% gelatin), with ($\sim 7 \times 10^7$ microbubbles/ml) and without microbubbles and in the absence of flow (Fig. 2). Prior to sonication, the microbubbles were distributed uniformly throughout the tunnel [Fig. 2(a)]. Application of ultrasound stimulated the acoustic particle cloud to move through the fluid, accumulate on the distal tissue surface, and deform the surface [Figs. 2(b) and 2(c)]. The deformation was spread laterally approximately 1 mm along the tissue interface on either side of the lateral centre of the ultrasound beam profile [Figs. 2(c) and 2(d)]. Removal of the acoustic field allowed the tissue to return to its normal geometry [Fig. 2(e)]. Without the presence of microbubbles in the tunnel, no (or low) tissue deformation was observed [Figs. 2(f)–2(j)]. The progressive change in optical contrast distribution is due to the movement of microbubbles away from the focal volume (see the videos for 1.2% and 2.5% gelatin phantoms in the supplementary material[16]). Ultrasound exposure produced a large displacement (100.6 ± 4.6 μm) in the presence of microbubbles (t: 0–6 ms) at the beginning of the pulse length [Fig. 2(k)]. As the microbubbles moved away from the focus, the displacement decreased (t: 6–16 ms). As the microbubble concentration at the focus decreased further, the displacement was reduced further (t: 16–40 ms) until it returned to normal when ultrasound was turned off (t: 40–60 ms).

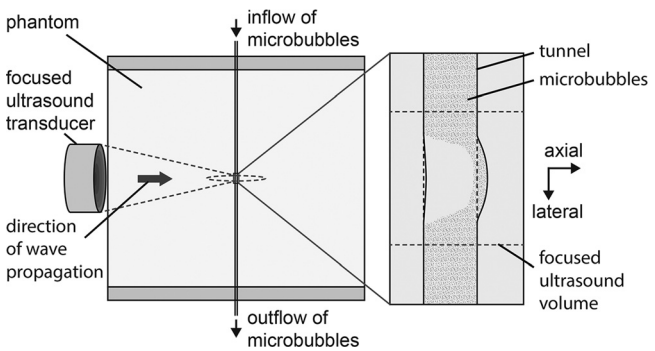

FIG. 1. Experimental setup. A phantom box containing a wall-less tunnel (diameter: 800 μm) immersed in a water tank was sonicated by a 5 MHz focused ultrasound transducer. Ultrasound pulses forced microbubbles against the tissue wall to cause a transient deformation that was monitored by high-speed optical microscopy (*right rectangular area*).

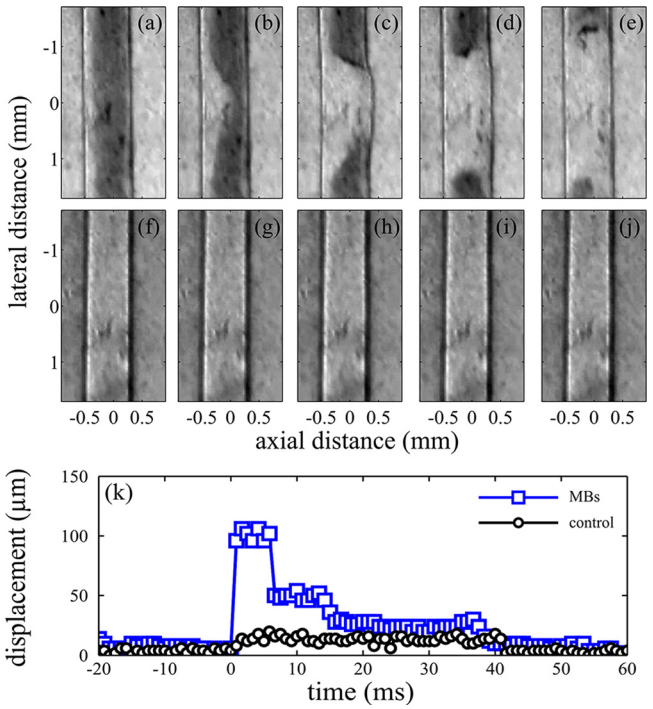

FIG. 2. Feasibility of acoustic particle palpation. A high-speed camera imaged a small area within the ultrasound region of exposure (Fig. 1). Ultrasound travelled left to right and was focused onto a volume that overlapped with a wall-less tunnel phantom (2.5% gelatin) containing microbubbles. Images were acquired 0, 0.83, 2.50, 8.3, and 40.8 ms after the start of the sonication (a–e) for microbubbles and (f–j) water alone inside the tunnel (f_c: 5 MHz, p_n: 625 kPa, PL: 40 ms). (k) The right wall deformation was tracked with (blue square) and without (black circle) microbubbles present. MBs: microbubbles, control: water alone.

In order to evaluate the relevance of this technique to biological tissue, we used a stiffer phantom material (5% gelatin) with a Young's modulus ($\sim$1.5 kPa) similar to liver and a lower microbubble concentration near the clinically recommended dose ($\sim 3 \times 10^6$ microbubbles/ml) that was made to flow through the tunnel using a syringe pump (flow rate: 1 ml/min). The deformation of a wall-less tunnel exposed to ultrasound [p_n: 625 kPa, PL: 20 ms, pulse repetition frequency (PRF): 2.5 Hz, number of pulses (N_p): 6] was determined for microbubbles and water only (Fig. 3). Without the presence of microbubbles in the tunnel, low tissue displacement (<1.5 μm) was observed. However, when microbubbles were administered, a higher net displacement (e.g., 11.8 ± 3.3 μm at $t = 5.83$ ms) was observed in the direction of wave propagation [Fig. 3(a)]. The deformation magnitude increased with peak-negative pressure [Fig. 3(b)]. We estimated the force magnitude based on the elastic properties of the material and deformation values by assuming the elastic medium to be isotropic, homogeneous, incompressible, and inviscid and considering the microbubble cloud as a single sphere indenting upon the interface (supplementary material[16]). An estimated force of 10 μN was obtained for a peak-negative pressure of 800 kPa when microbubbles were used, which has been previously shown sufficient to create a deformation that is detectable using ultrasound imaging methods.[8] Similar values were calculated using the Hertz theory (supplementary material[16]), which was employed here to describe the contact between a sphere (i.e., the microbubble cloud) and an elastic half-space (i.e., the channel-gelatin

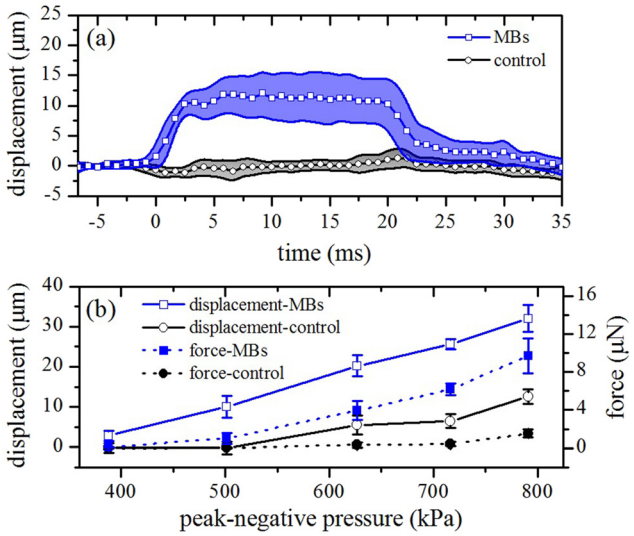

FIG. 3. Displacement at the palpation site. (a) Wall deformation of a wall-less tunnel phantom (5% gelatin) were tracked with (blue square) and without (black circle) microbubbles during exposure to ultrasound (f_c: 5 MHz, p_n: 625 kPa, PL: 20 ms, PRF: 2.5 Hz, N_p: 6). (b) The maximum displacement was measured and force values were estimated for different acoustic pressures. MBs: microbubbles, control: water alone.

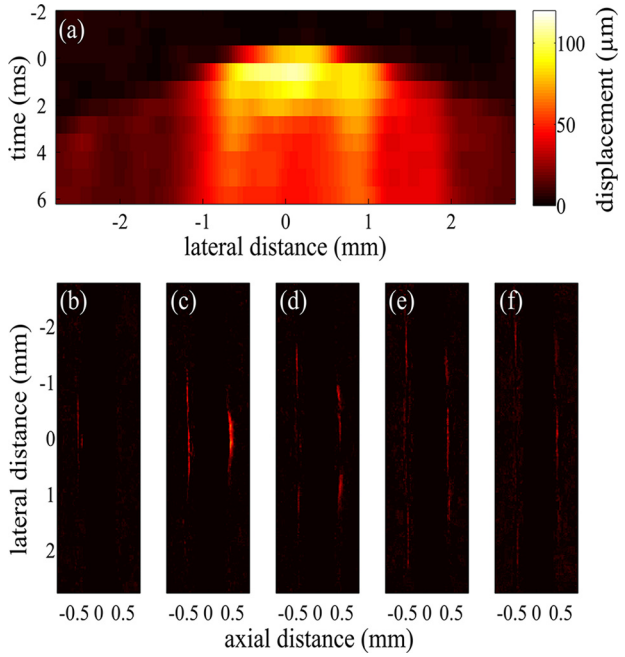

FIG. 4. Shear wave propagation away from the palpation site. A wall-less tunnel in a 2.5% gelatin phantom contained microbubbles and was exposed to ultrasound (f_c: 5 MHz, p_n: 625 kPa, PL: 40 ms). (a) Tissue displacement along the wall occurred within the focal volume and then spread away from the palpation site. (b–f) The subtraction of two successive images depict shear waves generated first on the proximal wall and then along the distal wall at $t = 0$, 0.83, 2.50, 3.33, and 4.2 ms.

interface). For example, an estimated force of 16 μN was obtained for a peak-negative pressure of 800 kPa when microbubbles were present.

Many ARF-based elasticity measurement techniques characterise the shear waves that propagate away from the excitation site.[6,17] Amongst the diverse properties characterised, the shear wave speed is the most prolifically measured, because it provides a quantitative estimate of elasticity. Imaging methods relying on compressional waves such as ultrasound can therefore be used to record propagation of shear waves, which propagate with speeds that are several orders of magnitude slower than those of compressional waves. In order to characterise the shear wave propagation, we measured the displacement along the tunnel wall for 2.5% gelatin phantom when exposed to ultrasound (f_c: 5 MHz, p_n: 625 kPa, PL: 40 ms) in the presence of microbubbles [Fig. 4(a)]. Immediately after ultrasound was applied, shear waves were observed to propagate away from the focal volume [Fig. 4(a)], which was also confirmed using subtraction of two successive images [Fig. 4(b)]. Interestingly, shear waves were first generated at the proximal wall, possibly due to the movement of the microbubble cloud away from it [Fig. 2(b)]. The shear wave velocity and Young's modulus were calculated to be $v_s = 0.39 \pm 0.03$ m/s and $E = 0.46 \pm 0.06$ kPa for a 2.5% gelatin phantom and $v_s = 0.71 \pm 0.07$ m/s and $E = 1.54 \pm 0.32$ kPa for a 5% gelatin phantom, assuming incompressible materials (Poisson's ratio: 0.5). These estimates are in good agreement with the reported values in the literature, extrapolated to our parametric region (i.e., $E = 0.1$–0.5 and 0.8–2.9 kPa for 2.5 and 5% gelatin, respectively).[18,19] No clear shear wave generation was observed in the control experiments for either the proximal or distal walls, thus indicating that palpation by ARF alone using the same ultrasound parameters is insufficient.

We have demonstrated the feasibility of using a population of microbubbles as a stress source for elasticity imaging. Acoustic particle palpation could enable localised elasticity measurements for a diverse range of clinical applications, such as the diagnosis of atherosclerosis,[20] fibrosis,[21] heart failure,[22] and cancer,[23] and non-clinical applications, such as material characterisation of tissue scaffolds, and other soft materials.

For a palpation method to be successful, it needs to generate enough displacement that can be tracked and imaged. In the clinic, ARF-based elasticity imaging methods, which do not use microbubbles, require a displacement of 1–10 μm for it to be tracked by ultrasound imaging.[8] Our results show that a 12-μm displacement is obtained in the presence of microbubbles at a low concentration ($\sim 3 \times 10^6$ microbubbles/ml) and low peak-negative pressure ($\sim$600 kPa). The palpation method here generates a larger force than ARF only techniques and the force is applied only to the surface of interest (i.e., fluid-tissue interface). This has the potential to improve the contrast of elasticity imaging. In our demonstration, the size of the palpation site was on the same order of magnitude as the ultrasound beam width, but a lower size may be achievable if the distribution of microbubbles is rearranged (e.g., as clusters) due to secondary ARF interactions. Here, we used optical microscopy to detect the tissue deformation, but other techniques such as ultrasound imaging or magnetic resonance imaging could be used to track the deformation response.

The general principle applied here is to use acoustic particle clouds that are displaced by ultrasound at a far higher magnitude than the surrounding material. We achieved this effect using microbubbles by matching the centre frequency of the ultrasound to the resonance frequency of the microbubbles to maximise primary ARF effects. Although the primary and secondary ARF effects are well established for a single

isolated microbubble,[24,25] the dynamics of acoustically driven microbubble clouds are not yet understood due to the complexity of the many-body bubble-bubble interactions.[26] Elucidating the underpinning mechanisms that lead to microbubble cloud movement through a fluid under long-pulse sonication and further understanding its mechanical interaction with the material interface is part of our future work.

Our demonstration of acoustic particle palpation can be incorporated into the diverse and broad range of excitation modes (transient, quasi-static, harmonic, etc.[8]), material tracking locations (on-axis,[5] off-axis[11]), and tracking algorithms (shear wave dispersion,[27] supersonic shear imaging,[17] etc.) developed over the last several decades for different imaging methods (ultrasound,[8] MRI,[3] etc.). In addition, although we used lipid-shelled microbubbles, which are clinically approved as an intravascular ultrasound contrast agents, it may be possible to use other particles (e.g., scattering agents) to produce the same effect.

In the clinical setting, acoustic particle palpation could be used to determine tissue elasticity wherever microbubbles are present. Microbubbles are currently being used as contrast agents in ultrasound imaging and are administered via an intravenous injection. The body's systemic circulation distributes the microbubbles throughout the body but they remain within the blood vessels as they are flowing. Non-invasive application of ultrasound would induce acoustic particle palpation from within the vessels, thereby allowing palpation of arteries, veins, arterioles, venules, and capillaries. Microvessels are a special case, because they have very thin vascular walls and take on the elastic properties of the surrounding microenvironment.[28] Thus palpation of microvessels could measure the soft tissue's mechanical properties. Microbubbles or other acoustic particles could also be administered into the lymphatic system via subcutaneous injections, cerebrospinal fluid, and fluid bodies, such as cysts. Application of ultrasound would then be able to probe these different tissue types.

The results presented here demonstrate that materials can be deformed using a population of acoustic particles and sound. We have shown that this is achieved by a multi-step process: ultrasound pushes microbubbles through fluid, the microbubbles press against the distal tissue surface, and the tissue deforms due to the application of this force. This method was repeated for biologically relevant ultrasound parameters and materials. The tissue deformation was on the order of microns and we have estimated the generation of force to be on the order of μNs. Finally, we have also demonstrated that this technique can be used to generate shear waves that are useful for tissue elasticity imaging. Acoustic particle palpation is a stress source that can enhance local elasticity measurements in different tissue environments and with a better resolution.

We would like to acknowledge the funding from the Wellcome Trust Institutional Strategic Support Fund to Imperial College London. H.K. was supported by the Scientific and Technical Research Council of Turkey (TUBITAK) in the context of the 2219-International Postdoctoral Research Fellowship Programme. A.G. was supported by the Qatar Foundation Research Leadership Programme (QRLP). We would like to thank Mr. Gary Jones for constructing the transducer holder, the phantom box, and the water tank.

[1]G. Binnig, C. Quate, and C. Gerber, Phys. Rev. Lett. **56**, 930 (1986).
[2]J. Ophir, I. Céspedes, H. Ponnekanti, Y. Yazdi, and X. Li, Ultrason. Imaging **13**, 111 (1991).
[3]R. Muthupillai, D. J. Lomas, P. J. Rossman, J. F. Greenleaf, A. Manduca, and R. L. Ehman, Science **269**, 1854 (1995).
[4]M. Fatemi and J. F. Greenleaf, Science **280**, 82 (1998).
[5]K. R. Nightingale, M. L. Palmeri, R. W. Nightingale, and G. E. Trahey, J. Acoust. Soc. Am. **110**, 625 (2001).
[6]S. A. Kruse, J. A. Smith, A. J. Lawrence, M. A. Dresner, A. Manduca, J. F. Greenleaf, and R. L. Ehman, Phys. Med. Biol. **45**, 1579 (2000).
[7]L. Sandrin, B. Fourquet, J.-M. Hasquenoph, S. Yon, C. Fournier, F. Mal, C. Christidis, M. Ziol, B. Poulet, F. Kazemi, M. Beaugrand, and R. Palau, Ultrasound Med. Biol. **29**, 1705 (2003).
[8]J. R. Doherty, G. E. Trahey, K. R. Nightingale, and M. L. Palmeri, IEEE Trans. Ultrason. Ferroelectr. Freq. Control **60**, 685 (2013).
[9]D. G. Grier, Nature **424**, 810 (2003).
[10]F. Mosconi, J. F. Allemand, D. Bensimon, and V. Croquette, Phys. Rev. Lett. **102**, 078301 (2009).
[11]A. P. Sarvazyan, O. V. Rudenko, S. D. Swanson, J. B. Fowlkes, and S. Y. Emelianov, Ultrasound Med. Biol. **24**, 1419 (1998).
[12]M. Friedrich-Rust, K. Wunder, S. Kriener, F. Sotoudeh, S. Richter, J. Bojunga, E. Herrmann, T. Poynard, C. F. Dietrich, J. Vermehren, S. Zeuzem, and C. Sarrazin, Radiology **252**, 595 (2009).
[13]A. Itoh, E. Ueno, E. Tohno, H. Kamma, H. Takahashi, T. Shiina, M. Yamakawa, and T. Matsumura, Radiology **239**, 341 (2006).
[14]T. N. Erpelding, K. W. Hollman, and M. O'Donnell, IEEE Trans. Ultrason. Ferroelectr. Freq. Control. **52**, 971 (2005).
[15]C. Acconcia, B. Y. C. Leung, K. Hynynen, and D. E. Goertz, Appl. Phys. Lett. **103**, 053701 (2013).
[16]See supplementary material at http://dx.doi.org/10.1063/1.4936345 for detailed explanation and multimedia files.
[17]J. Bercoff, M. Tanter, and M. Fink, Ultrason. IEEE Trans. Ferroelectr. Freq. Control. **51**, 396 (2004).
[18]C. Amador, M. W. Urban, S. Chen, Q. Chen, K.-N. An, and J. F. Greenleaf, IEEE Trans. Biomed. Eng. **58**, 1706 (2011).
[19]E. Mikula, K. Hollman, D. Chai, J. V. Jester, and T. Juhasz, Ultrasound Med. Biol. **40**, 1671 (2014).
[20]N. M. van Popele, D. E. Grobbee, M. L. Bots, R. Asmar, J. Topouchian, R. S. Reneman, A. P. Hoeks, D. A. van der Kuip, A. Hofman, and J. C. Witteman, Stroke **32**, 454 (2001).
[21]M. Ziol, A. Handra-Luca, A. Kettaneh, C. Christidis, F. Mal, F. Kazemi, V. de Lédinghen, P. Marcellin, D. Dhumeaux, J.-C. Trinchet, and M. Beaugrand, Hepatology **41**, 48 (2005).
[22]A. Borbély, J. van der Velden, Z. Papp, J. G. F. Bronzwaer, I. Edes, G. J. M. Stienen, and W. J. Paulus, Circulation **111**, 774 (2005).
[23]S. Suresh, Acta Biomater. **3**, 413 (2007).
[24]P. Dayton, K. Morgan, A. Klibanov, G. Brandenburger, K. Nightingale, and K. Ferrara, IEEE Trans. Ultrason. Ferroelectr. Freq. Control **44**, 1264 (1997).
[25]P. A. Dayton, J. S. Allen, and K. W. Ferrara, J. Acoust. Soc. Am. **112**, 2183 (2002).
[26]Z. Zeravcic, D. Lohse, and W. Van Saarloos, J. Fluid Mech. **680**, 114 (2011).
[27]S. Chen, M. Fatemi, and J. F. Greenleaf, J. Acoust. Soc. Am. **115**, 2781 (2004).
[28]Y. C. Fung, B. W. Zweifach, and M. Intaglietta, Circ. Res. **19**, 441 (1966).